Delivery of Antibacterial Nanoparticles into Dentinal Tubules Using High-intensity Focused Ultrasound

Annie Shrestha, BDS, MSc, Siew-Wan Fong, PhD,† Boo-Cheong Khoo, PhD,‡§ and Anil Kishen, BDS, MDS, PhD**

Abstract

Introduction: High-intensity focused ultrasound (HIFU) produces collapsing cavitation bubbles. This study aims to investigate the efficacy of collapsing cavitation bubbles to deliver antibacterial nanoparticles into dentinal tubules to improve root canal disinfection. **Methods:** In stage 1, experiments were performed to characterize the efficacy of collapsing cavitation bubbles to deliver the miniature plaster beads into a tubular channel model. In stage 2, experiments were conducted on root-dentin blocks to test the efficacy of HIFU applied at 27 kHz for 2 minutes to deliver antibacterial nanoparticles into dentinal tubules. After the stage 2 experiment, the samples were sectioned and analyzed using field-emission scanning electron microscopy and energy dispersive X-ray analysis. **Results:** The stage 1 experiment showed that collapsing cavitation bubbles using HIFU delivered plaster beads along the entire length of the tubular channel. It was observed from the stage 2 experiments that the diffusion of fluids alone was not able to deliver antibacterial nanoparticles into dentinal tubules. The collapsing cavitation bubbles treatment using HIFU resulted in significant penetration up to 1,000 μm of antibacterial nanoparticles into the dentinal tubules. The statistical analysis showed a highly significant difference in the depth of penetration of antibacterial nanoparticles between the two groups (<0.005). **Conclusion:**The cavitation bubbles produced using HIFU can be used as a potential method to deliver antibacterial nanoparticles into the dentinal tubules to enhance root canal disinfection. *(J Endod 2009;35:1028–1033)*

Key Words

Cavitation, dentinal tubules, nanoparticles, tubule penetration, ultrasonic

Ultrasound is applied in dentistry for the mechanical debridement of plaque and calculus (1–3). It has been applied for cutting dental hard tissues during cavity preparation and cleaning and shaping of the root canals. In addition, ultrasonics are used for the removal of intracanal materials, broken instruments, posts and metal cones, and in endodontic surgery to remove the apical root structure (4). Ongoing research interests in the application of ultrasound in dentistry include ultrasonic removal of dental biofilm (5, 6) and stimulation of odontoblast for the therapeutic application in dentin repair (7). The basic principle behind the application of ultrasound is the formation of cavitation bubbles (2, 8, 9). These bubbles are in a nonequilibrium state and will oscillate and collapse. The bubble dynamics involved is often complex because of the proximity of the nearby tissues (10). The forceful bubble collapse with high-speed jetting could be harnessed beneficially (as in the removal of biofilm) or could cause undesirable collateral damage (as in hard- and soft-tissue damages) (11).

Bacteria have been confirmed as one of the main etiologic factors of primary as well as persistent endodontic infections (12–14). The success of root canal treatment may depend on the complete elimination of microbes from the infected root canal system and the prevention of recolonization of microbes within the treated root canal system (15). The treatment of an infected root canal involves disinfection of the root canal system by a chemomechanical approach as well as interappointment medication. Nevertheless, microorganisms are known to resist conventional disinfection procedures after root canal treatment (14, 16, 17). The inability to completely disinfect root canal system has been attributed to the anatomic complexities of the root canal system and the structure of dentin (14).

Dentin structure is characterized by the presence of dentinal tubules traversing the entire bulk. The diameter of these tubules varies with the largest diameter toward the inner pulpal surface (0.5-4 μm), which narrows toward the DEJ or cementum. Bacterial presence in the dentinal tubules has been associated with persistent root canal infection (18). Studies have shown that bacteria can penetrate into dentinal tubules, and the depth of penetration varies from 300 μm to 1,500 μm (19, 20). Unfortunately, the bacteria within the dentinal tubules are inaccessible to the conventional root canal irrigants, medicaments, and sealers because they have limited penetrability into the dentinal tubules (21–24). Although the application of ultrasound produced better results compared with syringe irrigation in cleaning and delivering irrigants into the anatomic complexities (3), ultrasonic irrigation did not debride the root canal system completely (25).

Nanoparticles are microscopic particles that have at least one dimension less than 100 nm. Chitosan (poly[1,4],-β-D-glucopyranosamine) is an abundant natural biopolymer derived by the deacetylation of chitin found in the exoskeleton of

From the *Department of Restorative Dentistry, National University of Singapore, Singapore; †Institute of High Performance Computing, Singapore; ‡Department of Mechanical Engineering, National University of Singapore, Singapore; and §Singapore-MIT Alliance, Singapore.

Supported by the National University of Singapore cross-faculty grant (grant no. R-224-000-034-123) and the Academic Research Fund grant (grant no. R-224-000-028-112).

Address requests for reprints to Dr Anil Kishen, Department of Restorative Dentistry, National University of Singapore, Lower Kent Ridge Road, Singapore 119704. E-mail address: rsdak@nus.edu.sg.

0099-2399/$0 - see front matter

doi:10.1016/j.joen.2009.04.015

crustaceans (26). Chitosan nanoparticles have been used in various fields in the treatment of bacterial biofilms as well as wound healing primarily because of their antimicrobial properties and biocompatibility (26, 27). Chitosan nanoparticles have also been applied in various fields of medicine and science such as a carrier for the delivery of drugs and gene *in vivo* to treat various systemic disease conditions (28–30). Chitosan in the nanoparticles form has been reported to have low levels of cytotoxicity (28, 29). These nanoparticles by virtue of their size can be delivered into complex anatomies. Chitosan nanoparticles have been shown to provide a significant improvement in the root canal disinfection by effectively eliminating the residual adherent and nonadherent bacteria as well as increasing the diffusion of antibacterial components from the root canal sealers (31).

High-intensity focused ultrasound (HIFU) is applied clinically to generate collapsing cavitation bubbles in fluids and tissues, which collapses with high-speed jets that can be used for drug delivery. Earlier experiments have applied collapsing cavitation bubbles dynamics to pump liquid from one side of a perforated plate to the other side (32, 33). In this investigation, the high-speed jetting of collapsing cavitation bubbles produced by HIFU has been tested for the delivery of antibacterial nanoparticles into the dentinal tubules. The antibacterial chitosan nanoparticles used in this study have an average size of between 80 to 120 nm, which is smaller than the dentinal tubule. The experiments were conducted in two stages. In stage 1, the experiment was performed to characterize the efficiency of collapsing cavitation bubbles to deliver particles through a channel. The stage 1 experiment aided in understanding the mechanism involved in the delivery of antibacterial nanoparticles into dentinal tubules. In stage 2, *in vitro* experiments were conducted to deliver antibacterial nanoparticles into the dentinal tubules.

Materials and Methods

Stage 1: Characterization Experiment

Figure 1*A* shows the schematic of the experimental setup for the characterization experiment. A 3.7-cm long acrylic block (Young's modulus, $E = 3$) was used in this experiment because the bubble dynamics is sensitive to the elasticity of the material in an ultrasound field (10). The acrylic block was held in place by a holder, and a tubular channel of 3.3 mm in diameter was made in the block with a drill. The refractive index of the acrylic block was similar to that of water, and, therefore, very little image distortion was observed (Fig. 2). This allowed the plaster beads (2-mm diameter, representing particles) present within the channel to be photographed clearly. Two electrodes made of thin copper wires of 0.11 mm were wound on two wires that were connected to a discharging circuit consisting of a charged capacitor of 3,300 μF (charged to 52 V). This capacitor was connected to switch via a charging circuit comprising a current source and a 1-kΩ resistor. A spark bubble of approximately 3- to 4-mm radius was generated at the crossing point of the electrodes when the discharging circuit was switched on after the capacitor was charged up to 52 V via the charging circuit. More details about the spark bubble circuit and experimental setup can be found in a previous publication (32). The bubble generated collapsed at the opening of the channel, thus propelling the plaster beads along the entire length of the channel.

Stage 2: HIFU To Deliver Antibacterial Nanoparticles into the Dentinal Tubules

Chitosan polymer (low viscosity) and sodium tripolyphosphate (TPP) were purchased from Sigma Aldrich (USA). All other chemicals used were of analytic grade. Chitosan antibacterial nanoparticles were synthesized by ionic gelation as described in the literature (30). In brief,

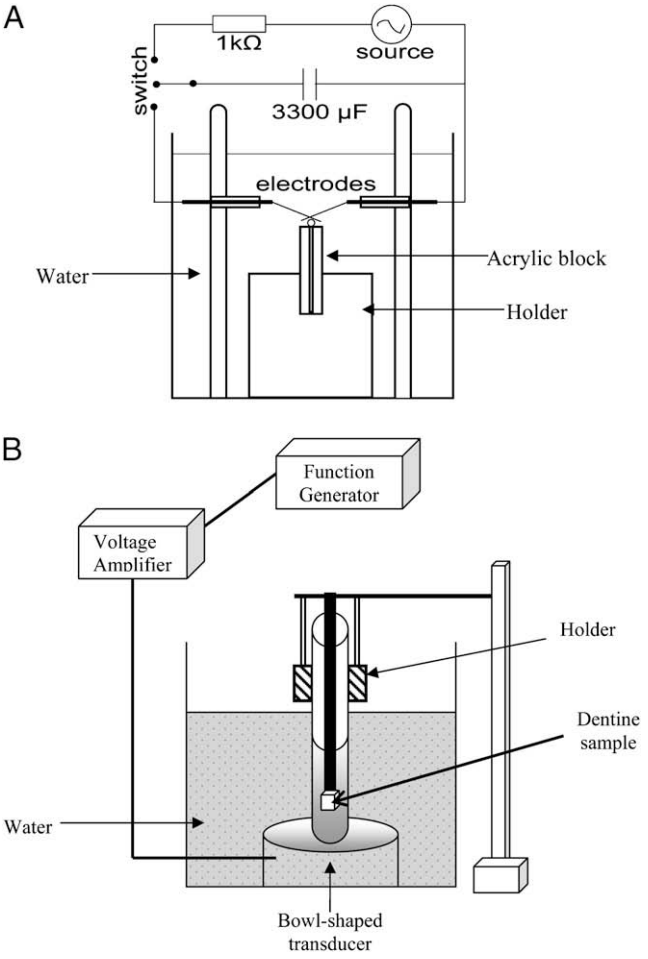

Figure 1. *(A)* HIFU experimental setup for the characterization experiment. The spark bubble was generated by discharging a capacitor which was charged to 52 V. More details of the spark bubble circuit can be found in Lew et al (32).The acrylic block (with a hole) was held at the water tank by a holder, and the plaster ball was placed right on top of the acrylic block below the crossing point of the electrodes (where the bubble was generated). *(B)* HIFU experimental arrangement used for *in vitro* experiments on dentine samples. The sample was attached by using adhesive glue to a glass rod and immersed into a test tube with antibacterial nanoparticles suspension. The test tube rested on the bowl-shaped transducer. High-intensity ultrasound was generated by the transducer, which was driven by the voltage amplifier at 126 V (with continuous 27-kHz sinusoidal signal from the function generator).

chitosan was dissolved in an acetic acid aqueous solution (0.1%) at the concentration of 1.2 mg/mL and TPP (1%) solution was prepared in distilled water. Chitosan and TPP were mixed (3:1 v/v) under magnetic stirring at room temperature. The solutions were centrifuged (15,000 rpm/20 minutes/18 °C) and washed twice in distilled water and freeze dried for 24 hours. The antibacterial-nanoparticles obtained ranged 80-120 nm in size as determined using field emission scanning electron microscopy (FESEM; JEOL, Tokyo, Japan). The experimental setup used in the study is shown in Figure 1*B*. FUS used in the study was generated by a disk ceramic transducer of 8.0 mm diameter at 27 kHz, with a driving voltage of about 126 V. The disk had a natural frequency of 2 MHz. It was driven by a voltage amplifier connected to a waveform generator. Sinusoidal wave of peak-to-peak amplitude 1.2 V and 27 kHz was used as a source. The disk rested on a brass holder that served

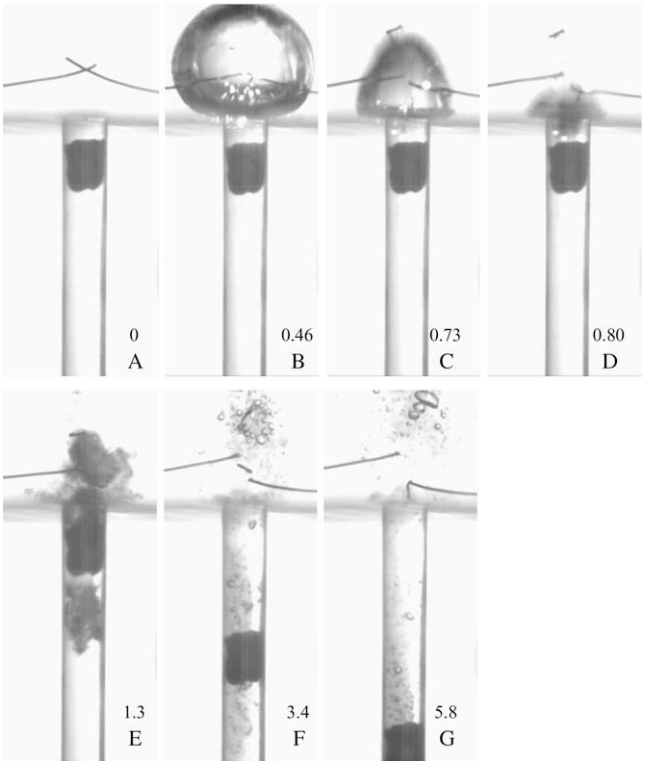

Figure 2. (*A-G*) The collapse of a spark discharge bubble of maximum bubble radius, R_{max} = 3.3 mm (taken horizontally from frame *B*, *t* = 0.46 milliseconds), on top of a tubular channel of 3.3-mm diameter. The timing for each frame in milliseconds; *t* is indicated at the bottom right. The bubble collapses at *t* = 0.73 *(C)* milliseconds with a jet speed of about 68/ms. The electrodes where the bubble is generated are placed 2.3 mm above the channel. The rubber plaster balls are centered initially 2 mm from the top of the channel opening. It can be seen from frame *t* = 1.3 to *t* = 5.8 ms; the rubber plaster is "pushed" by the flow down the entire length of the channel.

as a backrest for the transducer. Both the disk transducer and the holder were submerged in a water tank of about 15 × 15 × 15 cm^3.

Ten dentin sections from five intact human single-rooted teeth, free of cracks and caries extracted for periodontal reasons, were selected for this study. Teeth were sectioned at the cementoenamel junction, and the roots were taken for the study. Apical thirds were sectioned off to make all the sample length of approximately 8 mm. Roots were halved labiolingually with root canal in between. The root canal groove was flattened by using emery paper of grit sizes 600, 800, 1,200, and 4,000. The thickness and width of all the samples were maintained approximately at 1.5 mm and 3 mm, respectively. The flattened root canal surface was flushed with 2 mL of 17% EDTA followed by 2 mL of 5.25% sodium hypochlorite to remove the smear layer and expose the dentinal tubules. The 10 dentin sections were divided into two groups with five samples in each as follows: group 1: control group, dentin specimens immersed in antibacterial nanoparticles suspension without exposure to HIFU, and group 2: antibacterial nanoparticles group, dentin specimens immersed in antibacterial nanoparticles suspension and exposed to HIFU.

Antibacterial nanoparticles suspensions (2 mg/mL) were prepared in acetic acid aqueous solution (pH = 5) and ultrasonicated in the same HIFU setup for 1 minute for uniform dispersion. Teeth samples from group 1 were immersed in antibacterial nanoparticles suspension for 2 minutes. In case of HIFU exposure, samples from group 2 were immersed in antibacterial nanoparticles suspension with the dentinal tubular openings facing the ultrasonic plate at approximately 1.5 cm above the ultrasonic plate. The teeth samples were exposed to HIFU for 2 minutes. The samples were removed, stored in a desiccator, and subjected to FESEM and energy dispersive x-ray (EDX) analysis (JEOL). Vertical grooves were made using a slow-speed micromotor along the long axis of the root on the mesial and distal surface and split into two halves using a chisel, exposing the dentinal tubules. The samples were then platinum coated for 60 seconds and viewed under FESEM to ascertain the depth of penetration of the antibacterial nanoparticles within the dentinal tubules, whereas EDX analysis was used to determine the elemental concentration of the chitosan constituents to reconfirm the presence of antibacterial nanoparticles within dentinal tubules. During the analysis of the FESEM images, the depth of penetration of antibacterial nanoparticles into the dentinal tubules was categorized under three grades: grade 1 indicated the penetration of antibacterial nanoparticles to a depth of 500 μm from the root canal lumen, grade 2 indicated the penetration of antibacterial nanoparticles to a depth of 500 to 1,000 μm from the root canal lumen, and grade 3 indicated the penetration of antibacterial nanoparticles to a depth of more than 1,000 μm from the root canal lumen. The nanoparticles penetration was assessed for all the 10 samples, and grades of 1 to 3 were given depending on the depth of penetration. A paired *t* test was performed to evaluate the statistical significance with <0.05 as the significance level.

Results

Stage 1: Characterization Experiment

It was observed from this experiment that cavitation bubbles are formed all around the plaster bead when the HIFU was applied. The bubble grew to a maximum size with R_{max} (maximum radius) of 3.3 mm in 0.46 milliseconds time (*t*) (Fig. 2*B*). At this point of time, the bubble had overexpanded, resulting in a lower pressure inside the bubble than its environment causing the bubble to collapse as seen in the frame *t* = 0.80 milliseconds (Fig. 2*D*). The collapse of cavitation bubble generated a high-speed jet, which moved toward the channel at about 68/ms. This jet delivered the bead of plaster (5.8 mg), which was originally placed about 2 mm from the top of the channel, into the whole length of the channel (Fig. 2*E-G*).

Stage 2: HIFU To Deliver Antibacterial Nanoparticles Into the Dentinal Tubules

FESEM images of all the five samples from group 1 without the application of HIFU did not show the presence of antibacterial nanoparticles within the dentinal tubules and were scored as 0 (Fig. 3*A-C*). The openings of dentinal tubules toward the root canal lumen were also devoid of antibacterial-nanoparticles (Fig. 3*A*). The FESEM images of five dentin samples from the group 2 treatment group with HIFU exposure showed antibacterial nanoparticles penetration inside the dentinal tubules (Fig. 3*D-F*). The antibacterial nanoparticles were found to enter as deep as 1,000 μm into the dentinal tubules. Four out of five samples from group 2 were given grades of 2, and the remaining one was graded as 1 depending on the penetration of antibacterial nanoparticles. The statistical analysis showed a highly significant difference in the depth of penetration of antibacterial nanoparticles between the two groups (<0.005). The HIFU was not able to deliver nanoparticles to more than 1,000-μm deep. The antibacterial nanoparticles were seen as aggregates within the dentinal tubule lumen. However, the distribution of the antibacterial nanoparticles was not uniform within the dentinal tubule (Fig. 3*E*

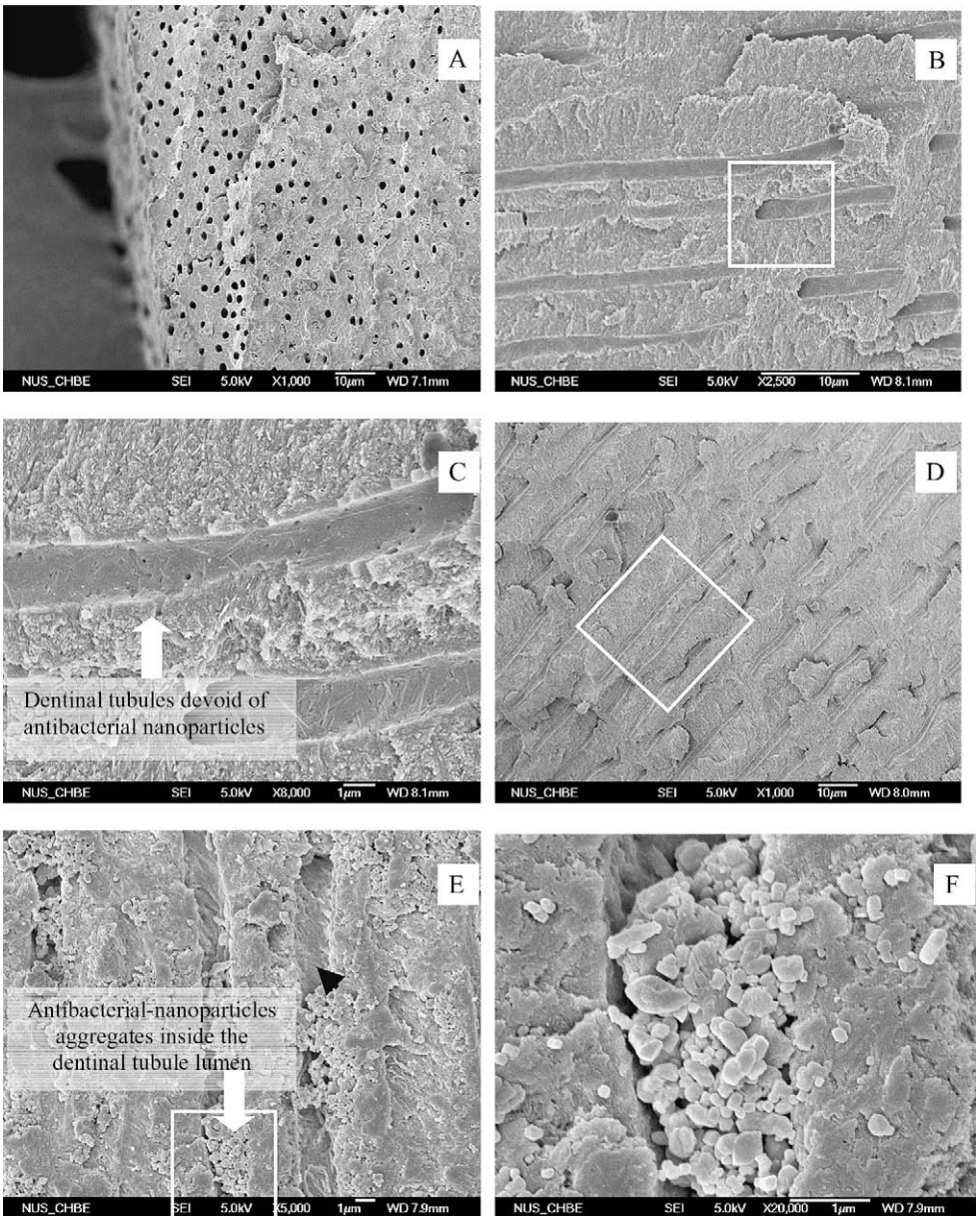

Figure 3. (*A-C*) Field emission scanning electron micrographs of a dentine sample from the control group without HIFU treatment. (*A*) The dentinal tubules opening toward the root canal wall is devoid of any antibacterial-nanoparticles attached to the surface. The cross-section of the dentine samples with exposed dentinal tubules does not show antibacterial-nanoparticles within the lumen (*B, C* magnified inlet from *B*). (*D-F*) Field Emission scanning electron micrographs of dentinal tubules from the HIFU treatment group sample. (*D*) A lower magnification view of dentinal tubules. The inlet in *D* is magnified in *E* showing antibacterial-nanoparticles penetrating into the dentinal tubules. The distribution of antibacterial-nanoparticles was found to be nonuniform along the lumen of the dentinal tubules (black arrow), and the nanoparticles showed a tendency to form aggregates (white arrow). A single dentinal tubule with antibacterial-nanoparticles within its lumen *(F)* showing aggregation of antibacterial nanoparticles of 100- $\pm$ 20-μm sizes.

and *F*). The ratio of nitrogen to carbon atomic mass percent obtained from the EDX spectrum was calculated. The dentin samples from the antibacterial nanoparticles treatment group with HIFU treatment showed higher nitrogen to carbon ratio (0.936) as compared with the dentin samples from the control group (0.512) without HIFU treatment (34).

Discussion

The ultrasonic system can produce two types of cavitations, one is a stable (noninertial) cavitation and the second is a transient (inertial) cavitation (35). Stable cavitations result from the linear pulsation of gas-filled bodies in a low-amplitude ultrasound field, which is mostly produced by dental ultrasonic system. In dental ultrasonics, transient cavitations occur only when the file can vibrate freely or with minimal contact within the canal (35, 36). The generation of inertial cavitation within the root canal depends on several factors. The files having a square cross-section and sharp edges produced significantly more inertial cavitations than a normal K file (35). In a curved canal, a preshaped file resulted in more inertial cavitation rather than a straight file (35). The ultrasonic irrigation of root canals has also been shown to be influenced

by canal taper, the application of irrigants, irrigation times, and the smoothness of the file used (6).

In case of transient or inertial cavitation, the gas bubbles undergo highly energetic pulsations. These inertial bubbles have been shown to collapse, radiating shockwaves and sufficient internal gas pressures to deliver particles into tubular spaces as observed in the characterization experiment (stage 1). When tested with dentin (stage 2), these bubbles collapsed when they came in contact with the dentinal surface, generating optimum internal gas pressure to deliver the antibacterial nanoparticles deep into the dentinal tubules. The penetration of antibacterial nanoparticles could be affected by the type of cavitation generated by the ultrasonic systems. Previous attempts to improve root canal disinfection by the use of ultrasonic systems showed limited benefits (25). This limitation can be attributed to several factors such as the type of bubbles or cavitations produced by the dental ultrasonic, the ability of the disinfectant to flow into the anatomical complexities and dentinal tubules, and the antimicrobial effect of the disinfectant. The cavitation produced by dental ultrasonics or endosonics are of both inertial and noninertial types. If noninertial cavitation occurs instead of the inertial type, the antimicrobial irrigants and antibacterial nanoparticles may not penetrate to the desired depth into the dentinal tubules. By using HIFU under the parameter used in this study, the penetration of antibacterial nanoparticles up to 1,000 μm into the dentinal tubules was observed, which can further improve root canal disinfection. To apply HIFU in endodontics, focused ultrasound should be generated intracanally. This can be achieved by using piezo ceramic crystal on the tip of a nonvibrating file or extracorporeal use of HIFU with the HIFU device touching only the tooth surface (37, 38). However, these aspects need to be investigated and thoroughly studied in future experiments.

Chitosan consists of amine groups that contribute to its nitrogen content (34). The higher ratio of nitrogen to carbon can be attributed to the presence of chitosan antibacterial nanoparticles within the dentinal tubules, which possess many nitrogen groups as observed from the EDX analysis (27). Chitosan is soluble only in acidic pH $\leq$ 6, and the antimicrobial effect has also been shown to decrease with increase in the pH (27, 39). In this study, chitosan antibacterial nanoparticles were dispersed in aqueous acetic acid solution. Because the acidic solution can induce demineralization effect on dental hard tissues, future experiments will be focused in using a water-soluble chitosan (such as quaternized chitosan) (40). The microscopic analysis showed that the distribution of antibacterial nanoparticles within dentinal tubules was not uniform and tended to aggregate. The study also showed that the diffusion of fluids alone was not enough to deliver antibacterial nanoparticles into the dentinal tubules, but additional forces in the form of collapsing cavitation bubbles were required. Earlier studies have shown the ability of antibacterial nanoparticles to disinfect root canal system by inhibiting bacterial adherence and improving the ability of root canal sealers to diffuse the antibacterial effect (31). The findings from this study showed the potential application of HIFU-generated collapsing cavitation bubbles to deliver antibacterial nanoparticles into the dentinal tubules and subsequently improve disinfection in endodontics.

References

1. . Repacholi MH, Benwell DA, eds. Essentials of medical ultrasound a practical introduction to the principles, techniques, and biomedical applications. Totowa, NJ: Humana Press; 1982.
2. Walmsley AD, Laird WR, Lumley PJ. Ultrasound in dentistry. Part 2–periodontology and endodontics. J Dent 1992;20:11–7.
3. Teplitsky PE, Chenail BL, Mack B, et al. Endodontic irrigation—a comparison of endosonic and syringe delivery systems. Int Endod J 1987;20:233–41.
4. Plotino G, Pameijer CH, Grande NM, et al. Ultrasonics in endodontics: a review of the literature. J Endod 2007;33:81–95.
5. Parini MR. Biofilm removal using bubbles and sound [master thesis]. Provo, UT: Brigham Young University; 2005.
6. van der Sluis LW, Versluis M, Wu MK, et al. Passive ultrasonic irrigation of the root canal: a review of the literature. Int Endod J 2007;40:415–26.
7. Scheven B, Millard J, Cooper P, et al. Short-term in vitro effects of low frequency ultrasound on odontoblast-like cells. Ultrasound Med Biol 2003;33:1475–82.
8. Leighton TG. The acoustic bubble. London: Academic Press Limited; 1994.
9. Lea SC, Price GJ, Walmsley AD. A study to determine whether cavitation occurs around dental ultrasonic scaling instruments. Ultrason Sonochem 2005;12: 233–6.
10. Fong SW, Klaseboer E, Turangan CK, et al. Numerical analysis of a gas bubble near bio-materials in an ultrasound field. Ultrasound Med Biol 2006;32:925–42.
11. Hill CR, Bamber JC, ter Haar GR. Physical principles of medical ultrasonics. West Sussex: John Wiley & Sons Ltd; 2004.
12. Kakehashi S, Stanley HR, Fitzgerald RJ. The effects of surgical exposures of dental pulps in germ-free and conventional laboratory rats. Oral Surg Oral Med Oral Pathol 1965;20:340–9.
13. Sundqvist G. Bacteriological studies of necrotic dental pulps [PhD thesis]. Umea, Sweden: University of Umea; 1976.
14. Nair PN, Henry S, Cano V, et al. Microbial status of apical root canal system of human mandibular first molars with primary apical periodontitis after "one-visit" endodontic treatment. Oral Surg Oral Med Oral Pathol 2005;99:231–52.
15. Bystrom A, Sundqvist G. Bacteriologic evaluation of the effect of 0.5 percent sodium hypochlorite in endodontic therapy. Oral Surg Oral Med Oral Pathol 1983;55: 307–12.
16. Bystrom A, Sundqvist G. The antibacterial action of sodium hypochlorite and EDTA in 60 cases of endodontic therapy. Int Endod J 1985;18:35–40.
17. Chugal NM, Clive JM, Spangberg LS. A prognostic model for assessment of the outcome of endodontic treatment: effect of biologic and diagnostic variables. Oral Surg Oral Med Oral Pathol 2001;91:342–52.
18. Siqueira JF, Uzeda MD. Disinfection by calcium hydroxide pastes of dentinal tubules infected with two obligate and one facultative anaerobic bacteria. J Endod 1996;22: 674–6.
19. Love RM, Jenkinson HF. Invasion of dentinal tubules by oral bacteria. Crit Rev Oral Biol Med 2002;13:171–83.
20. George S, Kishen A, Song KP. The role of environmental changes on monospecies biofilm formation on root canal wall by Enterococcus faecalis. J Endod 2005;31: 867–72.
21. Salzgeber RM, Brilliant JD. An in vivo evaluation of the penetration of an irrigating solution in root canals. J Endod 1977;3:394–8.
22. Vassiliadis LP, Sklavounos SA, Stavrianos CK. Depth of penetration and appearance of Grossman sealer in the dentinal tubules: an in vivo study. J Endod 1994;20: 373–6.
23. Peters OA, Schönenberger K, Laib A. Effects of four Ni–Ti preparation techniques on root canal geometry assessed by micro computed Tomography. Int Endod J 2001; 34:21–30.
24. de Paz LC. Redefining the persistent infection in root canals: possible role of biofilm communities. J Endod 2007;33:652–62.
25. Sequeira P, Fedorowicz Z, Nasser M, et al. Ultrasonic versus hand instrumentation for orthograde root canal treatment of permanent teeth. Cochrane Database Syst Rev 2007;17:CD006384.
26. Muzzarelli R, Tarsi R, Filippini O, et al. Antimicrobial properties of N-carboxybutyl chitosan. Antimicrob Agents Chemother 1990;34:2019–33.
27. Jung BO, Kim CH, Choi KS, et al. Preparation of amphiphilic Chitosan and their antimicrobial activities. J Appl Polym Sci 1999;72:1713–9.
28. Diebold Y, Jarrín M, Sáez V, et al. Ocular drug delivery by liposome-chitosan nanoparticle complexes (LCS-NP). Biomaterials 2007;28:1553–64.
29. Agnihotri SA, Nadagouda NM, Tejraj MA. Recent advances on chitosan-based micro- and nanoparticles in drug delivery. J Control Release 2004;100:52–8.
30. Shi Z, Neoh KG, Kang ET, et al. Antibacterial and mechanical properties of bone cement impregnated with Chitosan nanoparticles. Biomaterials 2006;27: 2440–9.
31. Kishen A, Shi Z, Shrestha A, et al. An investigation on the antibacterial and antibiofilm efficacy of cationic nanoparticulates for root canal disinfection. J Endod 2008;34: 1515–20.
32. Lew KSF, Klaseboer E, Khoo BC. A collapsing bubble-induced micropump: an experimental study. Sens Actuators A Phys 2006;133:16–72.
33. Dijkink R, Ohl C-D. Laser-induced cavitation based micropump. Lab Chip 2008;8: 1676–81.
34. Rabea EI, Badawy ME, Stevens CV, et al. Chitosan as antimicrobial agent: applications and mode of action. Biomacromol 2003;4:1457–65.
35. Roy RA, Ahmad M, Crum LA. Physical mechanisms governing the hydrodynamic response of an oscillating ultrasonic file. Int Endod J 1994;27:197–207.

36. Lumley PJ, Walmsley AD, Walton RE, et al. Cleaning of oval canals using ultrasonic or sonic instrumentation. J Endod 1993;19:453–7.
37. Shung KK, Cannata JM, Zhou QF. Piezoelectric materials for high frequency medical imaging applications: a review. J Electroceram 2007;19:139–45.
38. Wu J, Nyborg WLM. Emerging therapeutic ultrasound. Singapore: World Scientific; 2006.
39. Liu XF, Guan YL, Yang DZ, et al. Antibacterial action of chitosan and carboxymethylated chitosan. J Appl Polym Sci 2001;79:1324–35.
40. Verheul RJ, Verheul RJ, Amidi M, et al. Synthesis, characterization and in vitro biological properties of O-methyl free N, N, N-trimethylated chitosan. Biomater 2008;29:3642–9.